Supporting information

Micro-scale spatial location engineering of COF-TiO_2 heterojunctions for visible light driven photocatalytic alcohol oxidations

He Li,[a] Haoran Liu,[a,c] Chunzhi Li,[a,b] Jiali Liu,[a,b] Jian Liu,[a] Qihua Yang[a,*]

[a]State Key Laboratory of Catalysis, Dalian Institute of Chemical Physics, Chinese Academy of Sciences, Dalian 116023, China

[b]University of Chinese Academy of Sciences, Beijing 100049, China

[c]Key Laboratory of Theoretical Organic Chemistry and Functional Molecule (Ministry of Education), School of Chemistry and Chemical Engineering, Hunan University of Science and Technology, Xiangtan 411201, China

Corresponding author:

E-mail: yangqh@dicp.ac.cn (Q. Yang).

Characterizations

Liquid ^{1}H NMR spectra were recorded on a Bruker Avance 400 MHz spectrometer. Solid-state ^{13}C CP TOSS (total suppression of spinning sidebands) spectrum was tested on a Bruker 600 MHz spectrometer. FT-IR spectra in the range of 400 to 4000 cm^{-1} were collected with a Nicolet Nexus is50 IR spectrometer using KBr pellets. Powder X-ray diffraction (PXRD) patterns were recorded with a Rigaku RINT D/Max-2500 powder diffraction system using Cu Kα radiation. TGA was performed from 30 to 1000 °C with a heating rate of 5 °C min^{-1}, using a NETZSCHSTA 449F3 analyzer under air atmosphere. Nitrogen sorption isotherms were collected by using a Micromeritics ASAP 2020 system volumetric adsorption analyzer at 77 K. Before the sorption measurements, the samples were fully-degassed under 373 K for 6 h. The BET surface area was calculated from the adsorption data at a relative pressure P/P_0 in the range of 0.04 to 0.20. Pore size distributions were determined from the adsorption branch using a nonlocal density functional theory (NLDFT) method. TEM images were taken with a Hitachi 7700, at an acceleration voltage of 100 kV. Scanning electron microscopy (SEM) images were collected using a ZEISS SUPRA 55 field emission SEM. High-resolution scanning electron microscopy (HR-SEM) was undertaken by using a HITACHI S5500 apparatus operating at an acceleration voltage of 30 kV. FE-SEM-EDS elemental mapping was conducted by using a JSM-7900F field emission SEM. The photodeposition Pt nanoparticles was carried out by using a 300 W Xe lamp (Ushio-CERMAX LX300) and optical cutoff filter (kenko, L42; $\lambda \geq 420$ nm) for 3 hours with a Pt loading amount of 3 wt.% in 4 mL TEOA aqueous solution (15 vol%). STEM image and elemental mappings were taken on a JEOL JEM-ARM200F STEM. UV-vis absorption spectra were recorded on SHIMADZU UV-vis 2550 spectrophotometer. The photoluminescence (PL) spectra were conducted on a Fluoromax-4 spectrophotometer. The electrochemical impedance spectra (EIS), Mott-Schottky plots and photocurrent-time (I-T) profiles were measured by an electrochemical workstation (CHI660D, Shanghai, China) on a three-electrode system. In detail, Pt and saturated mercury electrode (SCE) electrode were used as counter electrode and reference electrode respectively, and Na_2SO_4 (0.2 M) was used as the electrolyte solution. A 300 W Xe lamp ($\lambda \geq 420$ nm) was used as the light source during the photocurrent-time (I-T) test. The EIS results were recorded over a frequency range of $0.01–10^5$

Hz with an amplitude of 6 mV at the same bias voltages. Electron paramagnetic resonance (EPR) spectra were collected on a Bruker EPR A200 spectrometer under air at 298 K.

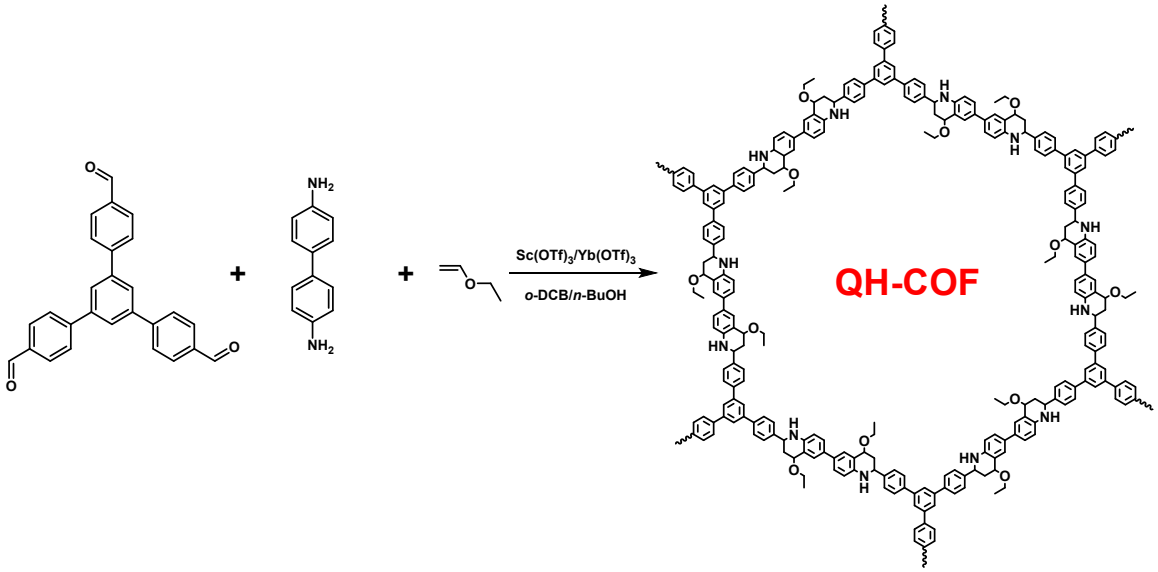

Scheme S1. Schematic illustration for the synthesis of QH-COF.

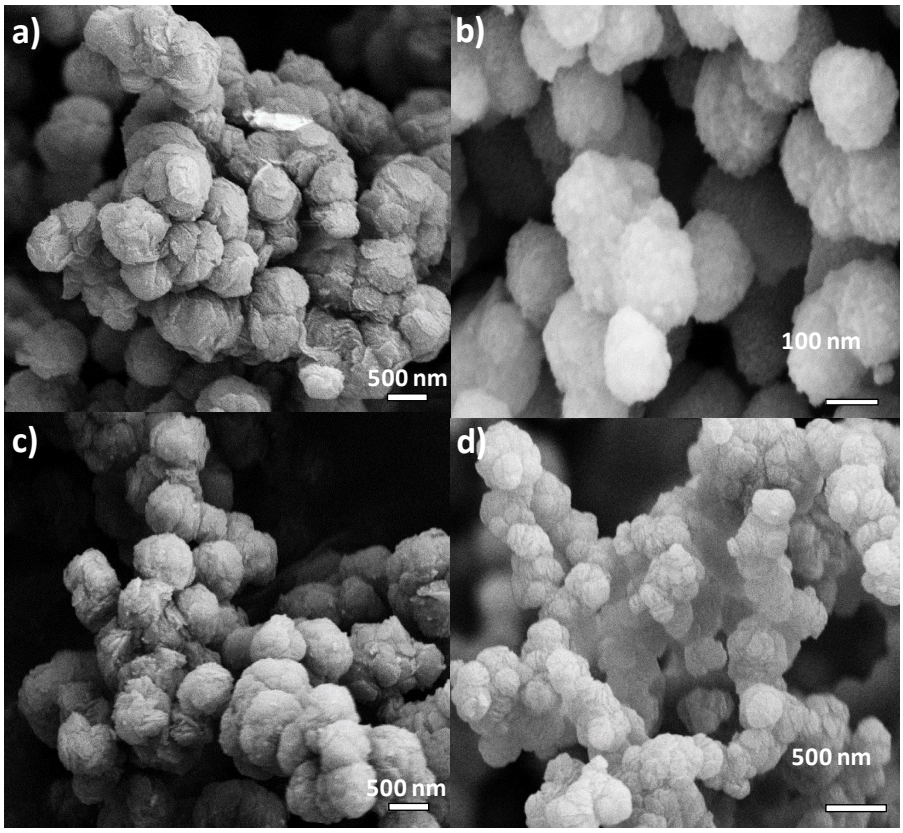

Figure S1. SEM images of (a) QH-COF, (b) TiO_2, (c) QH-COF@TiO_2(10%) and (d) TiO_2(10%)@QH-COF.

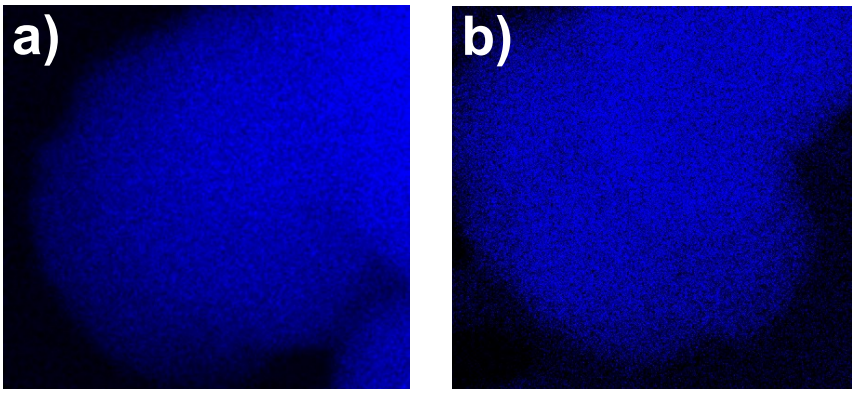

Figure S2. FE-SEM-EDS elemental mapping for C of (a) QH-COF@TiO_2(10%) and (b) TiO_2(10%)@QH-COF.

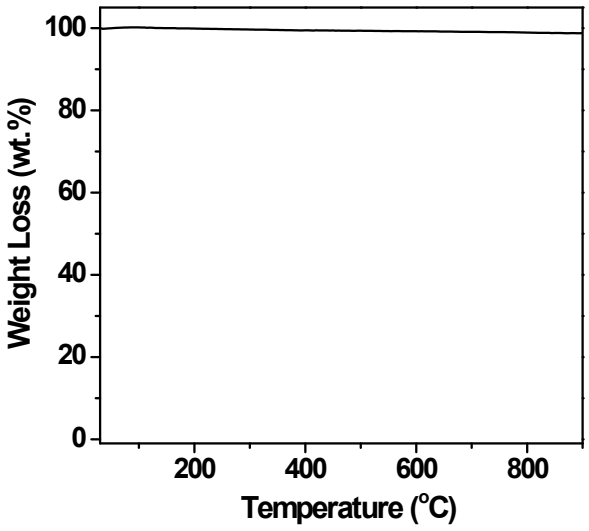

Figure S3. TGA curve of QH-COF@TiO_2(10%) after calcination in air (measured under air atmosphere).

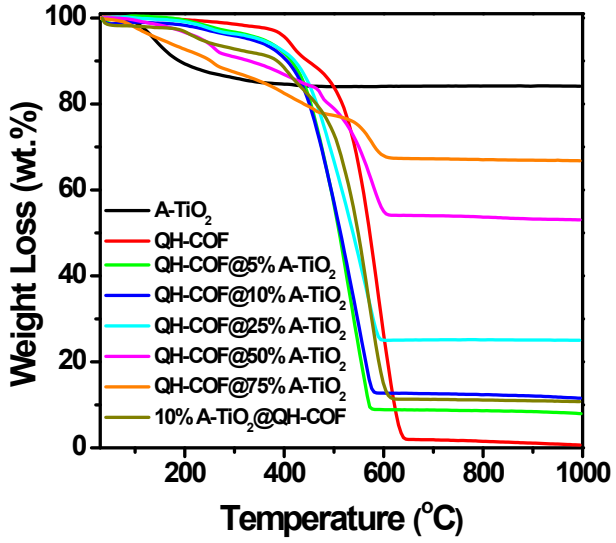

Figure S4. TGA curves under air atmosphere.

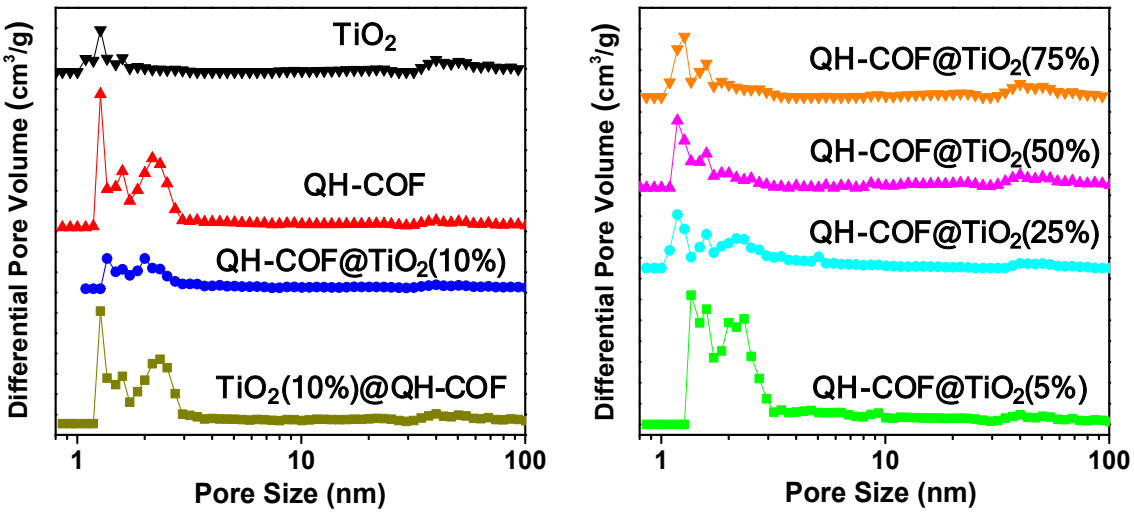

Figure S5. NLDFT pore size distribution curves.

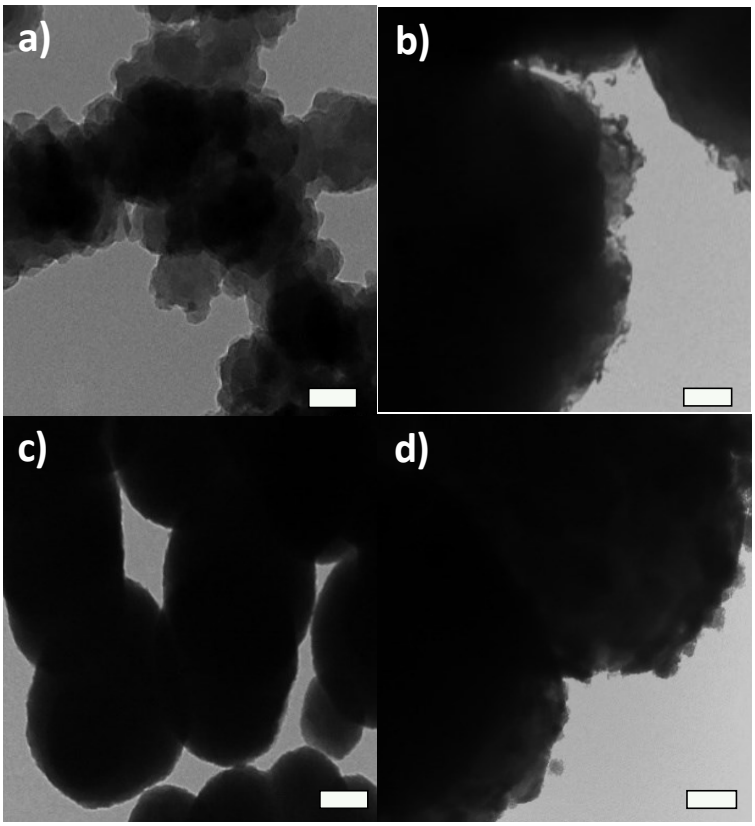

Figure S6. TEM pictures of (a) QH-COF@TiO_2(5%), (b) QH-COF@TiO_2(25%), (c) QH-COF@TiO_2(50%) and (d) QH-COF@TiO_2(75%) (Scale bar: 100 nm).

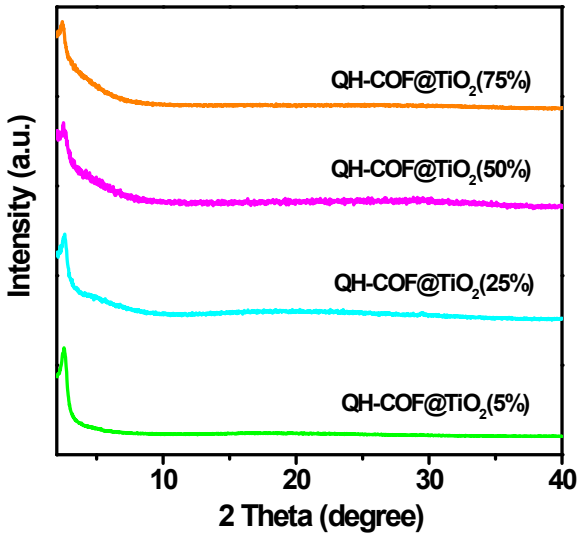

Figure S7. PXRD patterns of QH-COF@TiO_2 photocatalysts.

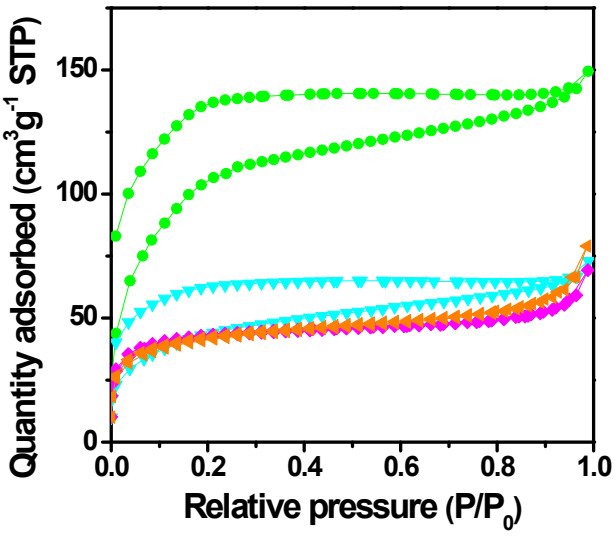

Figure S8. N_2 sorption isotherms of QH-COF@TiO_2(5%) (green), QH-COF@TiO_2(25%) (cyan), QH-COF@TiO_2(50%) (magenta) and QH-COF@TiO_2(75%) (orange).

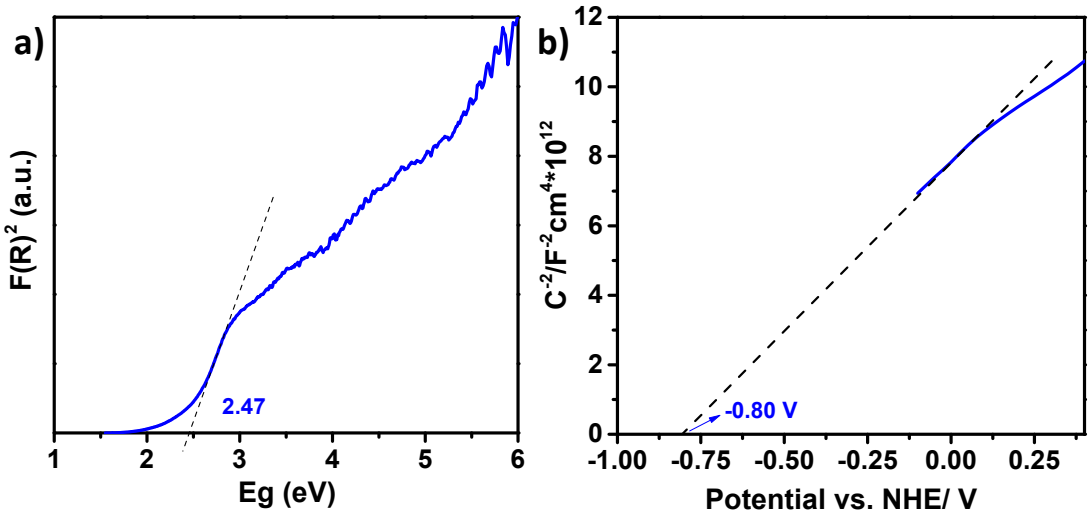

Figure S9. (a) Tauc plot and (b) Mott-Schottky plot of QH-COF@TiO_2(10%).

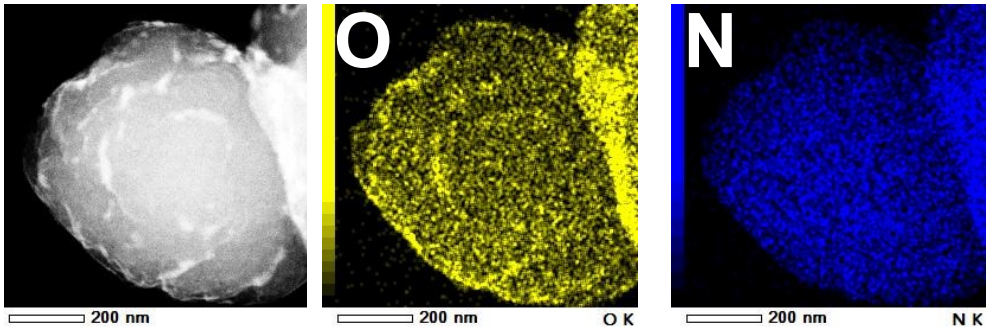

Figure S10. STEM image and elemental mappings of QH-COF@TiO_2(10%) after photo-deposition with Pt.

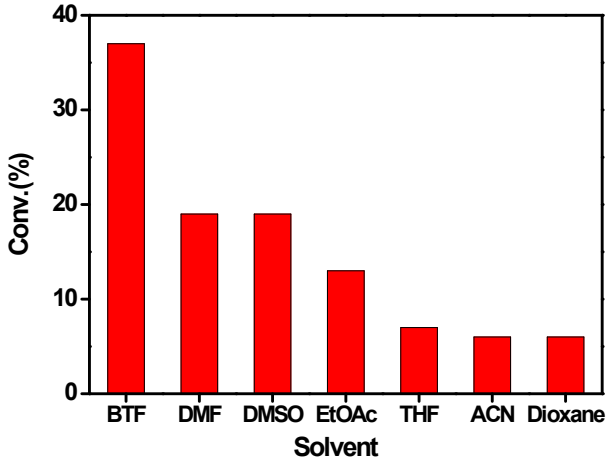

Figure S11. Visible light induced photocatalytic performance of QH-COF in oxidation for selective conversion of benzyl alcohol in different solvents. Reaction conditions: benzyl alcohol (0.05 mmol), Solvents (1 mL), QH-COF (16 mg), O_2 (1 bar), reaction time 2 h, 300W Xe lamp ($\lambda \geq 420$ nm).

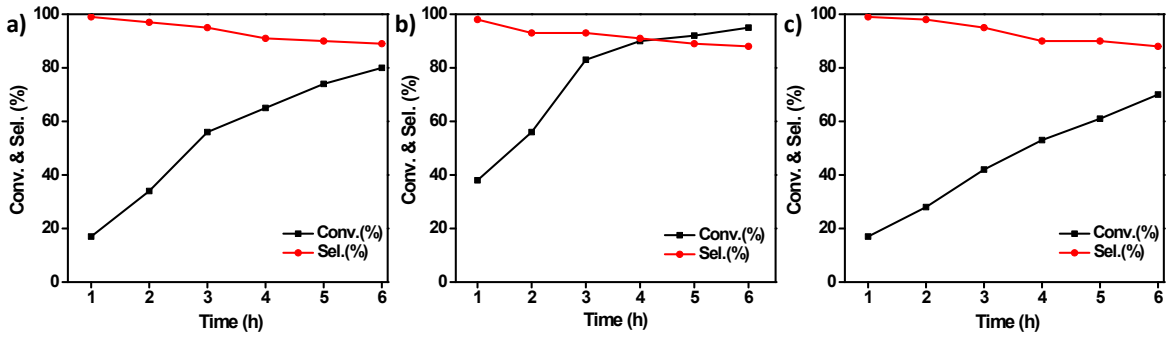

Figure S12. Kinetic curves for the photocatalytic oxidation of benzyl alcohol catalyzed by (a) QH-COF, (b) QH-COF@TiO_2(10%) and (c) TiO_2(10%)@QH-COF.

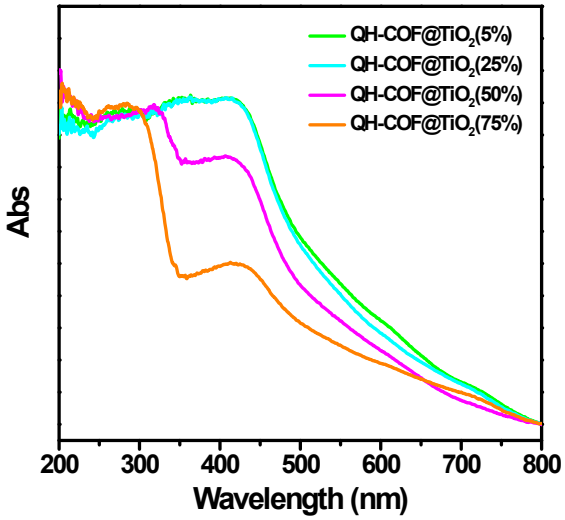

Figure S13. UV-vis diffuse reflectance spectra of QH-COF@TiO_2 photocatalysts.

Table S1. The comparison of results for the photocatalytic oxidation of benzyl alcohol activities over different COFs and MOFs reported in the literatures.

Photocatalyst	Solvent	Irradiance (nm)	Selectivity (%)	Reaction rate ($mmol \cdot g^{-1}h^{-1}$)	Ref.
QH-COF	BTF	≥ 420	95	0.58	This work
QH-COF@TiO_2(10%)	BTF	≥ 420	93	1.19	This work
NH_2-MIL-125-Ti	BTF	≥ 420	>99	0.075	S1
Ni-NH_2-MIL-125-Ti	BTF	≥ 420	>99	0.129	S1
MIL-100 (Fe)	Toluene	≥ 420	100	0.083	S2
MIL-125/C_3N_4	EtOH	> 400	93	0.93	S3
TAPB-PDA COF	ACN	> 420	>99	0.02	S4
NH_2-MIL-125@TAPB-PDA	ACN	> 420	>99	0.5	S4
Cu/Cu@UiO-66	ACN	≥ 400	>99	1.031	S5
UiO-66 (NH_2)	BTF	≥ 420	>99	0.66	S6
TiO_2@NH_2-MIL-125-Ti (LP-3)	BTF	≥ 420	99	0.21	S7
TiO_2@COF-3	ACN	> 420	>99	0.44	S8
CdS-UiO66	BTF	≥ 420	>99	0.94	S9

Table S2. CDC reactions of N-phenyl-1,2,3,4-tetrahydroisoquinoline over various catalysts.

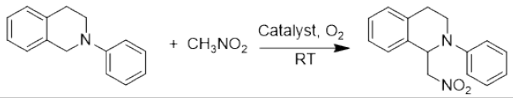

Catalyst	Light	Atmosphere	Yield (%)
QH-COF	-	O_2	5
\	+	O_2	\
QH-COF	+	N_2	13
QH-COF	+	O_2	53
TiO_2	+	O_2	10
QH-COF@TiO_2(10%)	+	O_2	81
TiO_2(10%)@QH-COF	+	O_2	73

Reaction conditions: N-phenyl-1,2,3,4-tetrahydroisoquinoline (0.2 mmol), nitromethane (2 mmol), methanol (4 mL), catalyst (10 mg), room temperature for 12 h, 1 bar of O_2, irradiation by a green LED lamp. The yield was determined by ^1H NMR spectroscopy using 1,3,5-trimethoxybenzene as an internal standard.

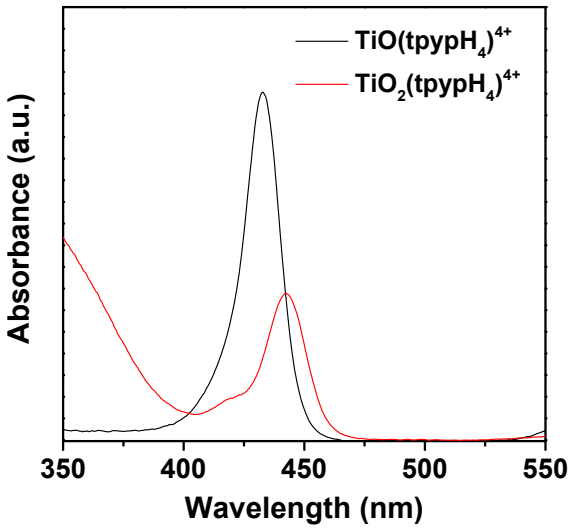

Figure S14. UV-vis spectra of fresh $TiO(tpypH_4)^{4+}$ and the mixture of $TiO(tpypH_4)^{4+}$ with the supernatant from the photocatalytic CDC reaction catalyzed by QH-COF@TiO_2(10%).

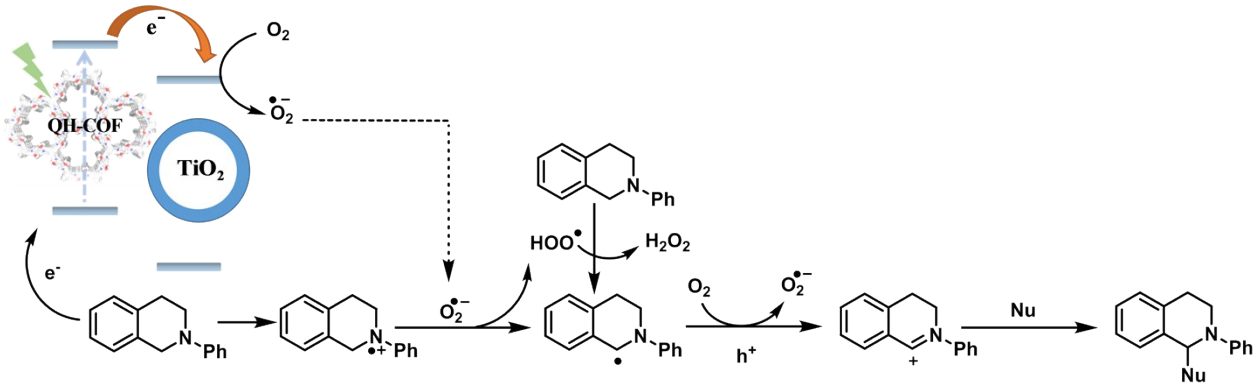

Scheme S2. Proposed mechanism for the photocatalytic aerobic CDC reaction of N-phenyl-1,2,3,4-tetrahydroisoquinoline and nucleophile in the presence of QH-COF@TiO_2(10%).

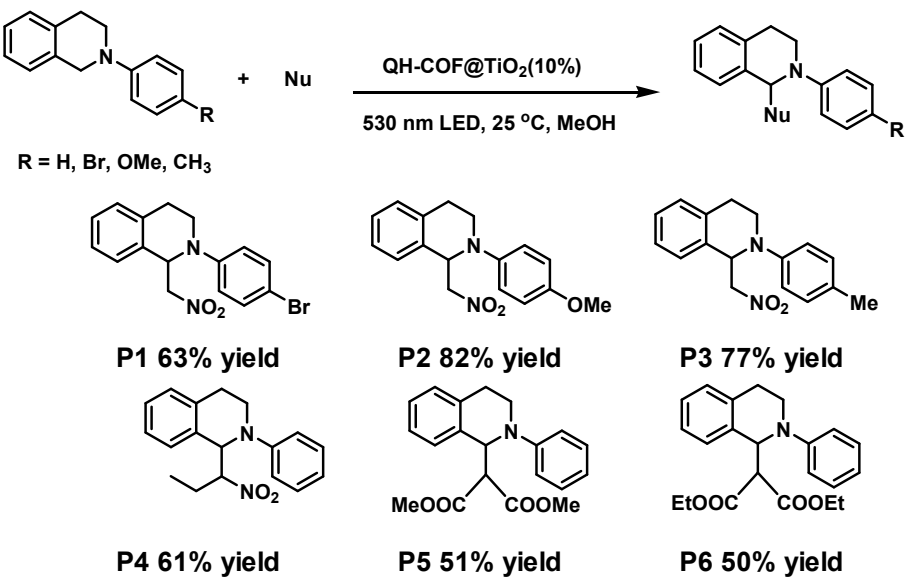

Figure S15. The substrate scope of photoreductive dehalogenation reactions over QH-COF@TiO_2(10%) (P1-P3: 12 h, P4-P6: 18 h).

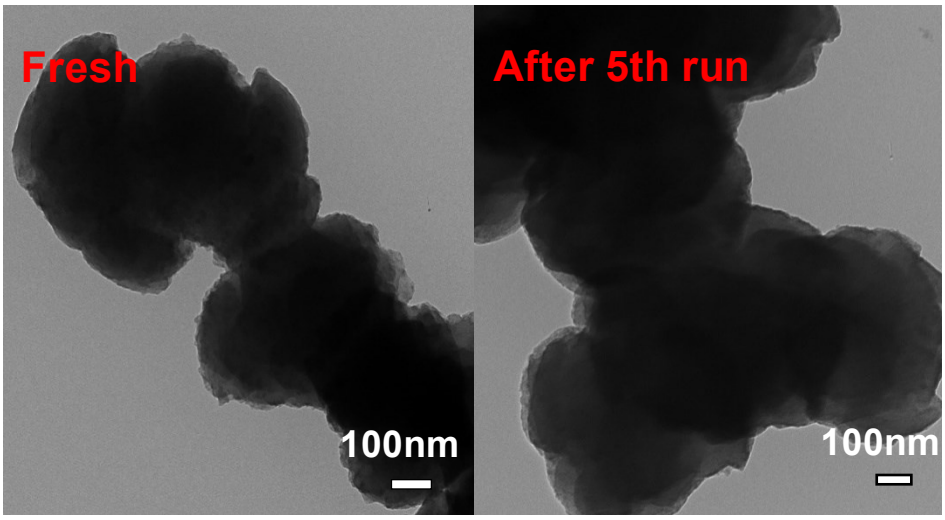

Figure S16. TEM images of fresh and recovered QH-COF@TiO_2(10%).

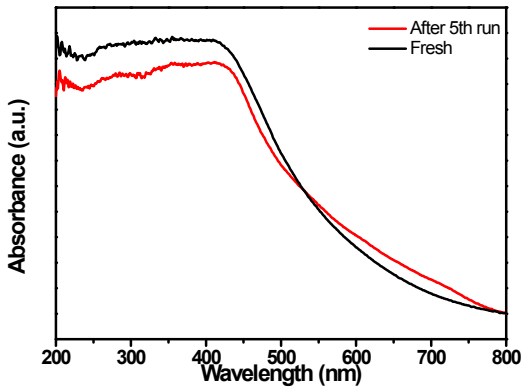

Figure S17. UV-Vis spectra of fresh and recovered QH-COF@TiO_2(10%).

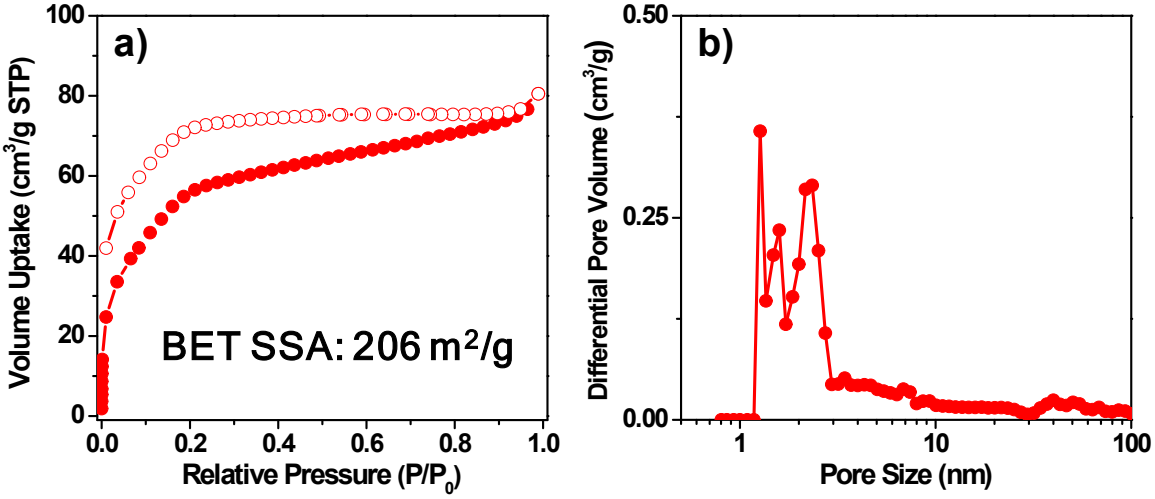

Figure S18. (a) N_2 sorption isotherms (measured at 77 K) and (b) NLDFT pore size distribution curve of recovered QH-COF@TiO_2(10%).

References for supporting information

[S1] Y. Fu, L. Sun, H. Yang, L. Xu, F. Zhang, W. Zhu, *Appl. Catal. B*, 2016, **187**, 212-217.

[S2] F. Ke, L. Wang, J. Zhu, *Nano Res.*, 2015, **8**, 1834-1846.

[S3] Z. Yang, X. Xu, X. Liang, C. Lei, Y. Cui, W. Wu, Y. Yang, Z. Zhang, Z. Lei, *Appl. Catal. B*, 2017, **205**, 42-54.

[S4] G. Lu, X. Huang, Y. Li, G. Zhao, G. Pang, G. Wang, *J. Energy Chem.*, 2020, **43**, 8-15.

[S5] L. Xiao, Q. Zhang, P. Chen, L. Chen, F. Ding, J. Tang, Y.-J. Li, C.-T. Au, S.-F. Yin, *Appl. Catal. B*, 2019, **248**, 380-387.

[S6] L. Shen, S. Liang, W. Wu, R. Liang, L. Wu, *Dalton Trans.*, 2013, **42**, 13649-13657.

[S7] X. Li, Y. Pi, Q. Hou, H. Yu, Z. Li, Y. Li, J. Xiao, *Chem. Commun.*, 2018, **54**, 1917-1920.

[S8] G. Lu, X. Huang, Z. Wu, Y. Li, L. Xing, H. Gao, W. Dong, G. Wang, *Appl. Surf. Sci.*, 2019, **493**, 551-560.

[S9] L. Shen, S. Liang, W. Wu, R. Liang, L. Wu, *J. Mater. Chem. A*, 2013, **1**, 11473-11482.